

Low Tuning Current Semiconductor Coupled-Cavity Lasers Incorporating Bragg Reflectors

Donald H. Brown, Michael B. Flynn, Liam O'Faolain, and Thomas F. Krauss

Abstract—Edge-emitting coupled-cavity semiconductor lasers employing a deeply etched Bragg reflector at one facet have been realized. The sidemode suppression ratio (SMSR) and wavelength tuning were investigated as a function of low level current injection. A single-mode tuning range of 3 nm centered around 977 nm displaying an SMSR better than 20 dB was obtained for tuning currents in the milliamper range.

Index Terms—Integrated optics, laser tuning, semiconductor lasers.

I. INTRODUCTION

CLEAVED coupled-cavity lasers have previously been reported [1], [2] as wavelength-tunable sources with high sidemode suppression. Traditional coupled-cavity devices consist of two or more optical cavities separated by air gaps sufficiently narrow to allow coupling of the optical wave between them. A change in the current flowing through either cavity changes that cavity's refractive index and, therefore, the cavity optical length. The total mode structure is subsequently modified; this is a simple and convenient method of spectral tuning. The operating mode of the compound device is determined by the interaction of the permitted modes from the individual sections and the coupling mechanism between them. Variations on these devices, involving the introduction of one- and two-dimensional photonic crystals, have recently prompted a renewed interest [3], [4] in coupled-cavity devices as either a possible alternative to more complicated tuned devices such as the sampled-grating distributed Bragg reflector (DBR) lasers or a viable method for developing a simple tunable laser with performance comparable to that of a distributed Bragg reflector DBR laser.

Advances in fabrication techniques permit the monolithic integration of coupled-cavity lasers with other on-chip functions, while addressing difficulties with fabrication tolerances and alignment [5], [6]. The purpose of this letter is to closely examine the tuning range and sidemode suppression ratio (SMSR).

II. FABRICATION

The coupled-cavity devices created for our work were fabricated from a GaAs–InGaAs double heterostructure (SCH) material wafer in which the active layer comprised a double quantum-well (DQW). The shallow active layer of 200 nm

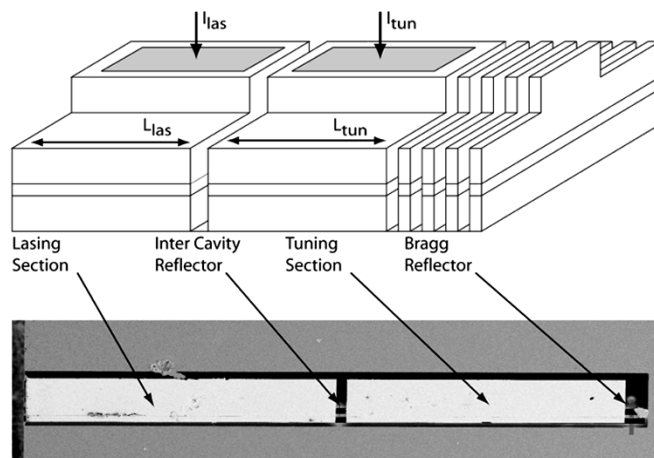


Fig. 1. Above: schematic of a typical coupled cavity laser, comprising two conventional DQW-SCH lasers separated by an intercavity reflector. One conventional cleaved facet has been replaced by a Bragg reflector. Below: scanning electron microscope of actual device with a Bragg reflector of six periods.

containing two InGaAs quantum wells of 75 Å was grown by metal–organic vapor phase epitaxy. We fabricated devices comprising two asymmetric cavities separated by intercavity reflectors (ICRs) of varying lengths. The structure of the fabricated devices including ICR and Bragg reflector is shown in Fig. 1.

Using a two-stage pattern transfer process, the deeply etched features of both the ICR and Bragg reflector were created. A combination of reactive ion etching and chemically assisted ion beam etching (CAIBE) ensures a feature-depth in excess of 1.2 μm. This is adequate to ensure that the two active layers are completely separated by the ICR, thus forming two independent cavities. The Bragg reflector also benefits from this etch depth through the reduction in coupling of light into the substrate modes. The reflector consists of six air slots spaced with a period of 510 nm. Using a simple transfer matrix method, the predicted wavelength range of operation is from 950 to 1100 nm, with a reflectivity approaching unity. Vertical side-walls are achieved by carefully balancing the CAIBE etching conditions [7]. ICR gap lengths of $L_g = \lambda, 1.5\lambda,$ and 2λ were investigated, where λ is the peak material gain wavelength of 980 nm. Slight variations due to fabrication tolerances resulted in a slot size variations. A slot size of 960 nm was found to provide the widest tuning range and best SMSR.

The longer of the two cavities, defined as the lasing section of the device, uses a cleaved facet as the output reflector. The length of this section was 300 μm after cleaving. The length of the tuning section is 280 μm and is accurately controlled by

Manuscript received February 2, 2005; revised June 15, 2005. This work was supported in part by Intense Photonics, Glasgow, U.K.

The authors are with the School of Physics and Astronomy, University of St. Andrews, St. Andrews, Fife KY16 9SS, U.K. (e-mail: tfk@st-andrews.ac.uk).

Digital Object Identifier 10.1109/LPT.2005.856371

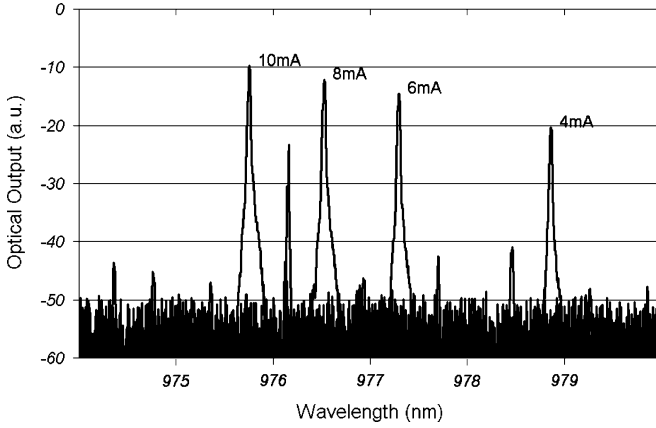


Fig. 2. Typical spectral output at selected tuning currents, while lasing current held at 10 mA. At higher modulation current, the wavelength of operation mode-hops back to 980 nm.

electron-beam lithography, which defines both the position of the ICR and Bragg reflector end mirror.

This cavity length difference of 20 μm ensures that there is sufficient gain threshold variation to obtain greater than 20-dB sidemode suppression, yet offering wavelength tunability. The Bragg reflector acts to create a high finesse tuning cavity resulting in an enhancement of the SMSR.

III. EXPERIMENTAL RESULTS

The devices were mounted p-side up on brass heat sinks and both sections tested individually, ensuring that the device was functional. Continuous-wave operation power–current characteristics were taken for the front cavity and typical threshold currents of 10 mA were achieved. Peak powers of 3 mW were observed. The devices were then probed in the coupled-cavity operation mode, and a single-mode optical fiber butt-coupled to the cleaved facet of the lasing section. An Ando AQ6317B optical spectral analyzer was used to capture the output spectra. The spectral properties of the coupled cavity lasers were measured under various operating conditions. Fig. 2 shows the optical spectra obtained for various currents applied to the tuning cavity with the lasing cavity operating with a current of 10 mA.

For a minimum SMSR of 20 dB, a tuning range of 942 GHz was measured with a corresponding tuning current range of 6.13 mA. As one would expect, this tuning range decreases as the minimum SMSR is increased. At 30 dB, the tuning range drops to 287 GHz for a tuning current range of 2 mA. Fig. 3 shows the minimum SMSR as a function of I_{tun} on the primary axis, while the wavelength of the laser output is presented on the secondary axis. From the measurements taken, a modal spacing of approximately 0.408 nm was obtained for the range of tuning currents tested. This modal spacing is in good agreement with theoretical predictions [8].

IV. DISCUSSION

A 4-nm blue shift was observed in the lasing spectra, which corresponds to a modal refractive index change of approximately 0.001. The nature of this shift confirms that the tuning is predominantly due to the effect of carrier injection.

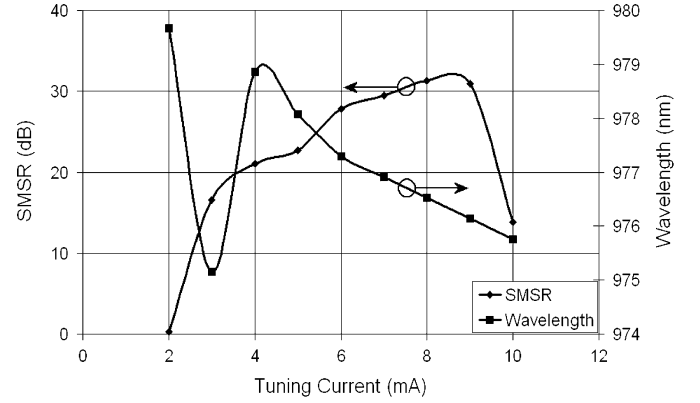


Fig. 3. Plot of SMSR (primary axis) and output wavelength (secondary axis) as a function of tuning current.

TABLE I
MODEL PARAMETERS [10]

Symbol	Description	Value
$\partial n/\partial N$	Differential of refractive index w.r.t. carrier density	$-2 \cdot 10^{-10} \text{ cm}^{-3}$
$\partial n/\partial \lambda$	Differential of refractive index w.r.t. wavelength	$-1 \mu\text{m}^{-1}$
η_i	Internal quantum efficiency	1.0
τ	Carrier lifetime	2 ns
d	Active layer thickness	250 nm
w	Active layer width	3 μm
n	Group Refractive index	4.5

Two separate phenomena contribute to carrier-induced refractive index change. The first is due to free carrier-plasma interaction, which is based on the Drude model of the polarizability of the electrons in an oscillating field. The second effect is a result of the change in gain or loss due to the injected carriers into the quantum wells and can be determined from the Kramers–Kronig relations. The carrier density in the active region is given by the formula

$$N = \frac{I\tau}{Ve} \quad (1)$$

where I is the current flowing into the cavity, τ is the carrier lifetime in the active region [8], V is the volume of the active region, and e is the charge of an electron. Following [9], we can combine these two effects discussed above, resulting in a phenomenological expression

$$\Delta n(N, \lambda) = \frac{\partial n}{\partial N} \frac{\eta_i I \tau}{Ve} + \frac{\partial n}{\partial \lambda} \Delta \lambda. \quad (2)$$

The final term is included to account for dispersion. A complete description of parameters and their values is given in Table I. Please note that the parameters were chosen for the best representation of the material used in the experiment and that there was no fitting parameter. The wavelength of the longitudinal mode m is given by

$$\lambda = \frac{2}{m} (n_{\text{las}} L_{\text{las}} + n_{\text{tun}} L_{\text{tun}} + n_{\text{Bragg}} L_{\text{Bragg}}) \quad (3)$$

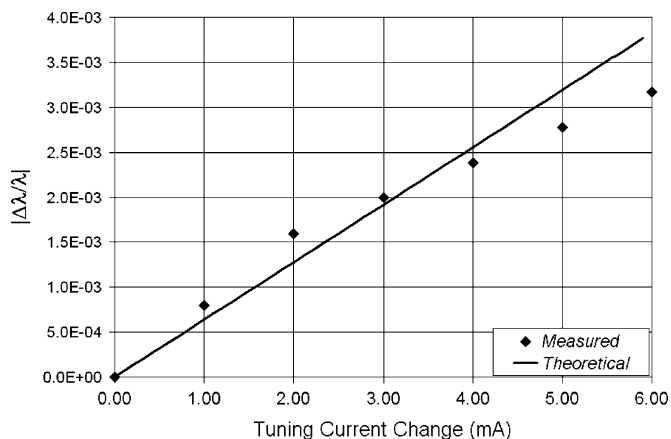


Fig. 4. Modeled magnitude of the wavelength shift versus tuning section current variations (4–10 mA) compared to experimental results.

where L_{Bragg} is the length of the Bragg reflector. By considering the effect of changing the refractive index in the tuning section and solving for the relative shift in mode m , we can approximate the relative wavelength tuning range from

$$\left| \frac{\Delta\lambda}{\lambda} \right| = \left| \frac{\Delta n_{\text{tun}} L_{\text{tun}}}{n_{\text{las}} L_{\text{las}} + n_{\text{tun}} L_{\text{tun}} + n_{\text{Bragg}} L_{\text{Bragg}}} \right|. \quad (4)$$

Fig. 4 demonstrates the relationship between the current to the tuning section and the wavelength shift of the device based on (2) and (4). For devices created with a lasing section length of $300 \mu\text{m}$, a tuning section of $280 \mu\text{m}$ and operating around 980 nm , the expected tuning range was 4–5 nm, which is in good agreement with the experimental data, especially since no fitting parameter was used.

Carrier injection offers a refractive index variation ($\Delta n/n$) with a switching speed of just a few nanoseconds. This is much faster than thermal tuning, which has a similar index variation but occurs on the time scale of a few milliseconds. As a result, switching times in coupled-cavity lasers can be expected to be below 10 ns, which has already been confirmed in previous studies [11], [12].

V. CONCLUSION

We have designed and fabricated a low power tunable coupled-cavity laser, possessing a tuning range over 942 GHz.

The simplicity of the fabrication involved suggests that this device could offer a cheaper alternative to more complex laser arrangements, e.g., as a wavelength-stabilized source via a suitable feedback loop. Although the device was exemplified in a DQW well III–V material operating at a wavelength of 977 nm , future work may employ a GaAs–InGaAs quantum-dot material structure capable of electroluminescence at $1.31 \mu\text{m}$. Investigation of devices from this new material is hoped to extend the suitability of this work in terms of the available tuning range. Overall, the coupled cavity approach offers increased SMSR and modest tuning range by very simple means.

REFERENCES

- [1] L. A. Coldren and T. L. Koch, "Analysis and design of coupled-cavity lasers—Part I: Threshold gain analysis and design guidelines," *IEEE J. Quantum Electron.*, vol. QE-20, no. 6, pp. 659–670, Jun. 1984.
- [2] W. Strieder, D. Yevick, T. L. Paoli, and R. D. Bernham, "An analysis of cleaved-cavity lasers," *IEEE J. Quantum Electron.*, vol. QE-20, no. 7, pp. 754–764, Jul. 1984.
- [3] S. Mahnkopf, M. Kamp, A. Forchel, and R. Marz, "Tunable distributed feedback laser with photonic crystal mirrors," *App. Phys. Lett.*, vol. 82, no. 12, pp. 2942–2944, May 2003.
- [4] S. Mahnkopf, R. Marz, M. Kamp, G. H. Duan, F. Lelarge, and A. Forchel, "Tunable photonic crystal coupled cavity laser," *IEEE J. Quantum Electron.*, vol. 40, no. 9, pp. 1306–1314, Sep. 2004.
- [5] L. A. Coldren, K. Furuya, B. I. Miller, and J. A. Rentschler, "Etched mirror and grooved-coupled GaInAsP/InP laser devices for integrated optics," *IEEE J. Quantum Electron.*, vol. QE-18, no. 10, pp. 1679–1687, Oct. 1982.
- [6] K. Avery, J. P. Reithmaier, F. Klopff, T. Happ, M. Kamp, and A. Forchel, "Deeply etched two-dimensional photonic crystals fabricated on GaAs/AlGaAs slab waveguides by using chemically assisted ion beam etching," *Microelectron. Eng.*, vol. 61, no. 62, pp. 875–880, 2002.
- [7] M. V. Kotlyar, L. O'Faolain, R. Wilson, and T. F. Krauss, "High aspect ratio chemically assisted ion beam etching for photonic crystals using a high beam voltage-current ratio," *J. Vac. Sci. Tech.*, vol. 22, pp. 1788–1791, 2004.
- [8] D. H. Brown, M. B. Flynn, L. O'Faolain, W. Sibbett, and T. F. Krauss, "Coupled cavity lasers incorporating Bragg mirrors," in *IEEE LEOS Meeting*, vol. 2, 2003, pp. 583–584.
- [9] M. B. Flynn, "Modeling of monolithic integrated semiconductor diode lasers as wavelength tunable and ultrashort pulsed sources," Ph.D. thesis, Univ. of St. Andrews, U.K., Oct. 2004.
- [10] L. A. Coldren and S. W. Corzine, *Diode Lasers and Photonic Integrated Circuits*. New York: Wiley, 1995.
- [11] K. J. Ebeling and L. A. Coldren, "Analysis of multielement semiconductor lasers," *J. Appl. Phys.*, vol. 54, pp. 2962–2969, 1983.
- [12] L. A. Coldren and T. L. Koch, "Analysis and design of coupled-cavity lasers—Part II; Transient analysis," *IEEE J. Quantum Electron.*, vol. 20, no. 6, pp. 671–682, Jun. 1984.